Eng. & Technology, Vol.24, No.8, 2005

Prediction of Laminar Flow and Heat Transfer in Axially Non-uniform Inner Annuli

Gazy F. Saloomy*
Received on: 30/5/2005
Accepted on: 25/10/2005

Abstract

Laminar flow and heat transfer in annular passages with axially nonuniform inner tubes were obtained numerically. A characteristic feature of these passages is that the flow separates in a stream wise direction. An axisymmetric coordinate system with an algebraic transformation in the radial direction has been used. Fully elliptic vorticity-stream function and energy equations in the transformed coordinates are solved using an iterative alternate direction implicit (ADI) method. In an annulus with a smooth blockage, the flow separates immediately downstream of the blockage at a Reynolds number of (1000). The heat flux is high in the constricted region. An increase in the heat transfer occurs where the fluid reattaches itself to the wall.

Keywords: Force convection axially non-uniform innor annuli

التنبؤ بجريان طباقي وانتقال الحرارة في قناة حلقية غير منتظمة من الداخل باتجاه الطول

الخلاصة

تم أجراء دراسة عددية لجريان طباقي وانتقال الحرارة في أنابيب ذات قناة حلقية غير منتظمة من الداخل باتجاه الطول. الخواص الأساسية لتلك القنوات هي إن الجريان يحدث به انفصال باتجاه الانسياب. تم استخدام نظام الاحداثي المتشابه مع التحول الجبري للإحداثيات الأصلية بالاتجاه القطري. حلت معادلات دوامية-دالة الانسياب والطاقة التفاضلية الاهليليجية المتكاملة مع الإحداثيات المتحولة باستخدام طريقة اختيار الاتجاه المباشر المتكررة. في القناة الحلقية وبوجود الحاجز الناعم، ظهر بان الجريان يحدث فيه انفصال بعد الحاجز مباشرة عند عدد رينولدز (1000)، وكذلك ظهر بان تدفق الحرارة يكون عالي في منطقة التضييق. ويحدث زيادة في انتقال الحرارة عندما يعود المائع لملامسة الجدار مرة أخرى.

* Dept. of Mechanical Eng., UOT, Baghdad-IRAQ.

https://doi.org/10.30684/etj.24.8A.17
2412-0758/University of Technology-Iraq, Baghdad, Iraq

Nomenclature

H	Maximum height of the blockage. (m)
h_w	Local heat transfer coefficient ($W/m^2.K$)
k	Thermal conductivity.(W/m.K)
L	Length of the blockage.(m)
L_t	Length of the computational domain.(m)
Nu	Local Nusselt number.
n	Normal to the wall.
Pe	Peclet number.
Pr	Prandtl number.
H	Height of the enclosure (m).
r	Radial coordinate.
$r_1(z)$	Inner tube radius.(m).
r_2^*	Outer tube radius.(m)
Re	Reynolds number.
T	Temperature (K).
u	Axial velocity.(m/s).
u_m	Mean axial velocity.(m/s)
v	Radial velocity.(m/s)
z	Axial coordinates.
Z_o	Distance of maximum blockage from the inlet.(m)
γ	Radial Ratio $(r_i(o)/r_2)$.
η	Transformed radial coordinate.
β	Transformed axial coordinate.
ψ	Stream function (m^2/s).
Ω	Vorticity.

Subscripts

1	Inlet.
2	Outlet.
i	Inner wall.
o	Outer wall.
w	Wall.

Superscripts

*	Dimensional quantity.

1. Introduction

Thermal hydraulic ducts of annular geometry is an important area of study for several engineering applications. Double-pipe heat exchangers, where two heat transfer fluids are separated by a tube wall, are commonly used. Annular passages are often studied to improve the basic understanding of flow and heat transfer in a nuclear rod bundle or a shell-and-tube heat exchanger. Heat transfer data for annuli are used in the design and performance evaluation of complex passages, where several hundred tubes may be arranged inside a shell. Due to operating conditions and design requirements, the flow cross section in these applications varies along the stream-wise direction. For example, in compact heat exchangers, extended surfaces are often introduced at the heat exchange boundary to enhance the surface to core area, and hence the heat transfer. In nuclear reactor cores, the fuel rods burst or swell due to high heat flux. The fuel rods may be locally damaged due to gas formation between the cladding and the fuel during the blow down phase of a loss of coolant accident. The knowledge of flow diversion and heat transfer in the blocked region is important to describe the response of the core during normal operation or the reflood phase of the accident.

Flow past a blockage has been studied for geophysical, heat transfer, biomedical and other applications. Ghia et al. [1] used a semi-elliptic model with conformal transformation to solve for laminar flow in a passage with two-dimensional contoured constriction. Parabolized momentum

equations along with an elliptic pressure equation were used. At a Reynolds number of (100), the flow separated only downstream of the constriction. At higher Reynolds number (1000), recirculation flow was obtained both upstream of the blockage and opposite the blocked wall. Rastogi [2] used a boundary fitted coordinate system to predict the flow in tubes with various types of axisymmetric blockages. Separation region behind a rounded obstruction was found to be less severe than the one behind a sharp-edged one.

A study of heat transfer in an annulus with a ring type blockage on the inner tube was conducted by Vilemas et al. [3]. Constant heat flux was applied on the tube with the blockage. Wall temperatures and Nusselt numbers upstream of the ring were the same as those in the smooth annulus. Immediately downstream of the obstacle, the wall temperature decreased sharply, and then increased gradually. Nusselt number immediately past the blockage was 2.5 times larger than that upstream of it. Thereafter, it decreased slowly to reach the fully developed value. Similar results were obtained by Drucker et al. [4] in a four-rod bundle with single and two-phase flows wherein sleeve type blockages mounted on each of the rods blocked 60% of the inner flow area.

In the present numerical study, flow and heat transfer in an annular passage with a smooth blockage on the inner tube are obtained by varying the geometric and the flow parameters. Geometric parameter is the height of the blockage. Flow parameters are the Reynolds number and the Prandtl number. The blocked tube is maintained at a constant temperature higher than the inlet temperature while the circular outer tube is insulated.

2. Mathematical model

Figure(1) shows the geometry and the coordinate system of a blocked annulus. The physical domain of interest is the annular gap. In the analysis, it is assumed that the flow area is symmetric in the transverse direction. Such an assumption limits the model to axisymmetric geometry.

Further assumptions are as follows:

1. The flow is laminar.
2. The fluid is Newtonian and incompressible.
3. Fluid Properties are constant. This is a valid assumption as long as temperature differences within the domain are not very high.
4. The viscous dissipation is negligible.

Navier-Stokes equations are expressed in the vorticity-stream function form. Steady-state results are obtained by marching in time. Therefore, although the model is valid for transient analysis, only the steady-state results are presented.

3. Governing Equations

Governing equations in an axisymmetric coordinate system are non-dimensionalized and can be written as [5]:

Vorticity transport equation:

$$\frac{\partial \Omega}{\partial t}+\frac{\partial}{\partial r}(v\Omega)+\frac{\partial}{\partial z}(u\Omega)+\frac{v}{r^2}\Omega=\frac{1}{\mathrm{Re}}\left(\frac{\partial^2\Omega}{\partial r^2}+\frac{\partial^2\Omega}{\partial z^2}+\frac{1}{r}\frac{\partial \Omega}{\partial r}-\frac{\Omega}{r^2}\right) \quad (1)$$

Vorticity definition equation:

$$\frac{1}{r}\frac{\partial^2\psi}{\partial r^2}+\frac{1}{r}\frac{\partial^2\psi}{\partial z^2}-\frac{1}{r^2}\frac{\partial\psi}{\partial r}=\Omega \quad (2)$$

Stream-function definition equations:

$$v=\frac{1}{r}\frac{\partial\psi}{\partial z} \quad (3)$$

$$u=-\frac{1}{r}\frac{\partial\psi}{\partial r} \quad (4)$$

Energy equation:

$$\frac{\partial T}{\partial t}+\frac{\partial}{\partial r}(vT)+\frac{\partial}{\partial z}(uT)+\frac{v}{r}T=\frac{1}{Pe}\left(\frac{\partial^2 T}{\partial r^2}+\frac{\partial^2 T}{\partial z^2}+\frac{1}{r}\frac{\partial T}{\partial r}\right) \quad (5)$$

Non-dimensional quantities in Eqs. (1)-(5) are defined as:

$$r=\frac{r^*}{r_2^*},\quad z=\frac{z^*}{r_2^*},\quad t=\frac{t^* u_m}{r_2^*}$$

$$v=\frac{v^*}{u_m},\quad u=\frac{u^*}{u_m}$$

$$\psi=\frac{\psi^*}{u_m r_2^*},\quad \Omega=\frac{\Omega^*}{u_m r_2^*}$$

$$\mathrm{Re}=\frac{u_m r_2^*}{\upsilon},\quad Pe=[\mathrm{Re}\,\mathrm{Pr}]$$

$$T=\frac{T^*-T_{o1}^*}{T_{i1}^*-T_{o1}^*}$$

4. Transformation

Since an axisymmetric coordinate system does not fit the irregular inner tube boundary, the radial coordinate is transformed algebraically so that the computational domain is rectangular. The transformation is given as [5]:

$$\eta=\frac{r-r_1(z)}{1-r_1(z)},\quad \beta=z \quad (6)$$

In the new coordinate system, $\eta=0.0$ at the inner tube wall, and $\eta=1$ at the outer tube wall. This holds well irrespective of the shape of the inner tube. Grid distribution in the physical and the computational domain is shown in Figure (2). The first-order gradient terms in the transformed coordinate system are:

$$\frac{\partial}{\partial r}=Co\left(\frac{\partial}{\partial\eta}\right) \quad (7)$$

$$\frac{\partial}{\partial z}=Cl\left(\frac{\partial}{\partial\eta}\right)+\frac{\partial}{\partial\beta} \quad (8)$$

Where Co and Cl are the geometric coefficients of transformation given as:

$$Co=\frac{1}{1-r_1(z)} \quad (9)$$

$$Cl=\left(\frac{\eta-1}{1-r_1(z)}\right)\frac{dr_1}{dz} \quad (10)$$

The second-order gradient terms in the new coordinate system are:

$$\frac{\partial^2}{\partial r^2}=Co^2\frac{\partial^2}{\partial^2\eta} \quad (11)$$

$$\frac{\partial^2}{\partial z^2}=\frac{\partial^2}{\partial\beta^2}+Cl^2\frac{\partial^2}{\partial\eta^2}+2Cl\frac{\partial}{\partial\eta\partial\beta}+\frac{\partial Cl}{\partial\beta}\frac{\partial}{\partial\eta}+Cl\frac{\partial Cl}{\partial\eta}\frac{\partial}{\partial\eta} \quad (12)$$

5. Transformed Equations

Using Eqs.(6)-(12), the transformed equations became as:

Vorticity transport equation:

$$\frac{\partial\Omega}{\partial t}+\frac{\partial}{\partial\eta}\left[(Co\,v+Cl\,u)\Omega-\Gamma_{\eta}\frac{\partial\Omega}{\partial\eta}\right]+\frac{\partial}{\partial\beta}\left(u\Omega-\Gamma_{\beta}\frac{\partial\Omega}{\partial\beta}\right)=b \quad (13)$$

Where, (Γ_{η}) and (Γ_{β}) are the diffusion coefficients in η and β directions respectively. Also (b) is the source term.

$$\Gamma_{\eta}=\frac{Co^2+Cl^2}{\mathrm{Re}} \quad (14)$$

$$\Gamma_{\beta}=\frac{1}{\mathrm{Re}} \quad (15)$$

$$b=\frac{1}{\mathrm{Re}}\left(\frac{Co\,\partial\Omega}{r\ \partial\eta}+\frac{\partial Cl}{\partial\beta}\frac{\partial\Omega}{\partial\eta}+Cl\frac{\partial Cl}{\partial\eta}\frac{\partial\Omega}{\partial\eta}+2Cl\frac{\partial^2\Omega}{\partial\eta\partial\beta}\right)-\frac{1}{\mathrm{Re}}\frac{\Omega}{r^2}-\frac{v}{r^2}\Omega \quad (16)$$

Energy equation:

$$\frac{\partial T}{\partial t}+\frac{\partial}{\partial\eta}\left[(Co\,v+Cl\,u)T-\Gamma_{\eta T}\frac{\partial T}{\partial\eta}\right]+\frac{\partial}{\partial\beta}\left(uT-\Gamma_{\beta T}\frac{\partial T}{\partial\beta}\right)=b \quad (17)$$

where, $(\Gamma_{\eta T})$ and $(\Gamma_{\beta T})$ are the diffusion coefficients in η and β directions respectively. Also (b) is the source term.

$$\Gamma_{\eta T}=\frac{Co^2+Cl^2}{Pe} \quad (18)$$

$$\Gamma_{\beta T}=\frac{1}{Pe} \quad (19)$$

$$b=\frac{1}{Pe}\left(\frac{Co\,\partial T}{r\ \partial\eta}+\frac{\partial Cl}{\partial\beta}\frac{\partial T}{\partial\eta}+Cl\frac{\partial Cl}{\partial\eta}\frac{\partial T}{\partial\eta}+2Cl\frac{\partial^2 T}{\partial\eta\partial\beta}\right)-\frac{v}{r}T \quad (20)$$

Vorticity definition equation:

$$A_1\frac{\partial^2\psi}{\partial\eta^2}+\frac{1}{r}\frac{\partial^2\psi}{\partial\beta^2}+B_1\frac{\partial\psi}{\partial\eta}+2\frac{Cl}{r}\frac{\partial^2\psi}{\partial\eta\partial\beta}=\Omega \quad (21)$$

Where A_1, B_1 are the geometric coefficients introduced due to the transformation, and are given as:

$$A_1=\frac{Co^2+Cl^2}{r} \quad (22)$$

$$B_1=\left(\frac{1}{r}\frac{\partial Cl}{\partial\beta}+\frac{Cl}{r}\frac{\partial Cl}{\partial\beta}-\frac{Co}{r^2}\right) \quad (23)$$

Stream function definition equations:

$$v=\frac{1}{r}\left(Cl\frac{\partial\psi}{\partial\eta}+\frac{\partial\psi}{\partial\beta}\right) \quad (24)$$

$$u=-\frac{Co}{r}\left(\frac{\partial\psi}{\partial\eta}\right) \quad (25)$$

6. Boundary conditions equations.

Solid walls:

Stream-function values at the walls are:

At $\eta=0.0$, $\psi=\psi_{i}=\frac{1-r_i^2(z)}{2}$ (26)

At $\eta=1$, $\psi=\psi_{o}=0.0$ (27)

Vorticity values at the walls are :

At $\eta=0.0$, $\Omega=\Omega_{i}=Al\frac{\partial^2\psi_{i}}{\partial\eta^2}$ (28)

At $\eta=1$, $\Omega=\Omega_{o}=Co\frac{\partial^2\psi_{o}}{\partial\eta^2}$ (29)

where $\frac{\partial^2\psi_{w}}{\partial\eta^2}=\frac{2(\psi_{w}-\psi_{w+1})}{(\Delta\eta)^2}$

The inner tube is maintained at a temperature higher than the inlet temperature. While the outer tube is insulated.

Inlet and outlet:
Stream-function at the inlet in transformed form is [5]:

$$\psi_1 = \psi_o + \int_0^1 \frac{u_1 r}{Co} d\eta \qquad (30)$$

Inflow condition for the vorticity is [5]:

$$\Omega_1 = A1 \frac{\partial^2 \psi_1}{\partial \eta^2} + B1 \frac{\partial \psi_1}{\partial \eta} \qquad (31)$$

At the outlet boundary condition in transformed domain:

$$\left.\frac{\partial \Omega}{\partial \beta}\right|_2 = \left.\frac{\partial \psi}{\partial \beta}\right|_2 = 0.0 \qquad (32)$$

$$\left.\frac{\partial^2 T}{\partial \beta^2}\right|_2 = 0.0 \qquad (33)$$

7. Solution procedure.

7.1 Finite-Difference Scheme.

Equations (13) and (17) are integrated over the control volume $(\Delta\eta\,\Delta\beta)$ as shown in Fig. (3), to obtain the finite difference form of vorticity transport and energy equations. Discretized equations

$$a_P X_P = a_E X_E + a_W X_W + a_N X_N + a_S X_S + b \qquad (34)$$

Where X corresponds to Ω or T, a_E, a_W, a_N, and a_S represent influence by convection and diffusion at the four faces of the control volume in terms of the flow rate and the conductance. The term b includes effects of the source term, cross-derivatives due to the transformation, and the time-dependent term. Finite-differencing has been done using the power-law scheme suggested by Patankar [6].

7.2 Solution Algorithm.

Steady-state solutions for the flow field and temperature distribution are obtained by marching in time. At each time step, coupled vorticity and stream-function equations are solved by an iterative procedure. Iterations are required to obtain correct vorticity boundary conditions, particularly at the start of the solution. The vorticity equation (13) is solved using the (ADI) method. The stream-function equation (21) is solved using the Gauss-Seidel iteration. Once the vorticity steady state is achieved, the energy equation is solved using the (ADI) method. The solution sequence is as follows:

1. Calculate geometric coefficients of transformation.
2. Initialize variables.
3. Solve the vorticity transport equation using the (ADI) method.
4. Iteratively solve the stream-function equation. The convergence is checked.
5. Update vorticity values at the walls.
6. Update velocities from stream-function definition equations.
7. Return to step 3 until vorticity steady-state has converged.
8. Solve the energy equation by the (ADI) method. Steady-state convergence is checked.

8. Results and discussions

The local Nusselt number is defined as:

$$Nu = \frac{h_w r_2^*}{k} \qquad (35)$$

Where the local heat transfer coefficient (h_w) is obtained from the local heat balance as:

$$h_w = \frac{-k\left(\partial T / \partial n\right)_w}{T_w - T_m} \qquad (36)$$

In this study, the inner tube radius is described by a normal distribution function such that [5]:

$$r_1(z) = \gamma + he^{-15(z-z_0)^2} \qquad (37)$$

8.1 Base conditions:

Flow and heat transfer in a blocked annulus of radius ratio γ=0.5 are obtained at the base conditions. These are: blockage height h=0.4, blockage length L=1.0, Re=1000, and Pr=1.0.Computations were performed with L_f=6.0, computational grids are (21 radial*121 axial).

Flow field: The flow and stream patterns at base conditions are shown in Fig. (4). Corresponding axial velocity profiles at the entrance, in the blocked region, and downstream of the blockage are shown in Fig. (5). It is seen that the flow is unaffected upstream of the blockage. As the blockage starts at (z=1.5), there is a slight increase in the axial velocity near the inner wall region. Thereafter, the fluid accelerates until it reaches the peak of the blockage. Because of reduction in the flow area in this region, main flow with a central core, having axial velocity 3 to 4 times higher than the inlet velocity, is established. As the flow area increases downstream of the maximum constriction, the flow separates simultaneously at both the walls. The separation occurs immediately past the maximum constriction (z-2.0) at a plane where (z=2.1). The main flow in this region is bounded by recirculation zones on both sides. The recirculation eddy near the outer wall is stronger and larger the recirculation eddy in the wake of the blockage. At (z=2.5), where the blockage ends, the axial velocity of the main flow is about twice that of the inlet velocity. This is because the main flow area is reduced due to the recirculation zones. Due to blockage the flow is diverted toward the inner wall where it attaches itself downstream of the eddy in the wake of the blockage.

Temperature field: Isotherms and local Nusselt numbers (normalized with respect to the value at the inlet) are shown in Figs. (6)-(7). It is seen that the effect of the blockage is not felt upstream of it. As the flow area decreases, the temperature gradient and hence the Nusselt number increase. Maximum heat transfer occurs at the maximum constriction. Thereafter, as the flow separates, the heat transfer decreases. This is due to the fact that the recirculation eddy in the wake of the blockage restricts the convective heat transfer from the wall.

8.2 Effect of flow parameters.

Reynolds number: Stream patterns at various Reynolds numbers are shown in Fig.(8). At a low Reynolds number of 10, the fluid diffuses uniformly around the blockage. No upstream or downstream effects are noticeable for

such highly viscous flows. At Re=100, the flow separates and an upstream recirculation eddy is formed. The flow pattern at Re=1000 shows that the flow separates and weak recirculation eddies are formed on both sides of the main flow. The flow pattern at Re=2000 is similar to that at Re=1000. However, the recirculation eddies on the outer wall and near the exit on the inner wall is bigger.

The local Nusselt number is shown in Fig.(9). This figure illustrates the effect of the Reynolds number on heat transfer from the inner wall. The heat transfer increases in regions close to the blockage. The increase is even more at higher Reynolds numbers.

Prandtl number: since the fluid properties are assumed to be constant, the flow field is not affected by the Prandtl number. Effect of the Prandtl number on heat transfer is shown in Fig.(10). As the Prandtl number increases, the heat transfer increases in the blocked region.

8.3 Effect of geometric parameters.

The geometric parameter studied is the height of the blockage at a Reynolds number of 1000 wherein the flow pattern is well established. Stream patterns for different block heights are shown in Fig.(11). About 15% reduction in the flow area, caused by a blockage with height (h=0.1) does not affect the flow. As the blockage increases to about 40% of the flow area (h=0.25), its influence is felt close to the inner wall only. The flow separates in the wake of the blockage. With further increase in the blockage height (h=0.4), the effect is felt near the outer wall also. Nusselt number ratio at the inner wall is shown in Fig.(12). Downstream of the blockage, the heat transfer increases as the blockage height increase. At (h=0.1), effects of the blockage are insignificant.

9. Conclusion.

A numerical model to predict flow and heat transfer in variable cross-sectional annular passages has been described. Fluid flow and heat transfer in annuli with smooth blockage on the inner tube, obstructing up to 75% of the flow area, have been obtained. It is found that the blockage does not affect the flow at low Reynolds numbers. At higher Reynolds numbers, the main features of the flow are established at Re=1000. Upstream effects of the blockage are small. At Re>100, the flow separates immediately downstream of the maximum constriction. Heat flux from the inner wall is high in the narrow regions. Heat transfer in the initial parts of the recirculation eddy is low. However, a sharp increase takes place at a location where the fluid attaches itself to the wall.

10. References.

1. Ghia U., Ghia K. N., Rubinn S. G.G., Khosla P. K., "Study of Incompressible Flow Separation Using Primitive Variables", Comput. Fluids, vol. 9, pp. 123-142,1981.

2. Rastogi A. K., "Hydrodynamics in Tubes Perturbed by Curvilinear Obstruction", ASMEJ. Fluids Eng., vol. 106, pp. 262-269, 1984.

3. Vilemas J., Cesna B., Survila V., "Heat Transfer in Gas-cooled Annular

Channels", eds. A. Zukauskas and J. Karni, pp. 134-139, Hemisphere, Washinton, D.C., 1987.
4. Drucker M. I., Dhir V. K., Duffey R. B., Ford G., Hagemeyer B., "Two-phase Heat Transfer in Tubes", ASME paper No. 82-WA/HT-47, 1982.
5. Agrawal A. K., Sengupta S., "Laminar flow and Heat Transfer in Blocked Annuli", Numer. Heat Transfer, part A, vol. 15, pp. 489-508, 1989.
6. Patankar S. V., "Numerical Heat Transfer and Fluid Flow", Chap. 5, Hemisphere, Washington, D.C., 1980.

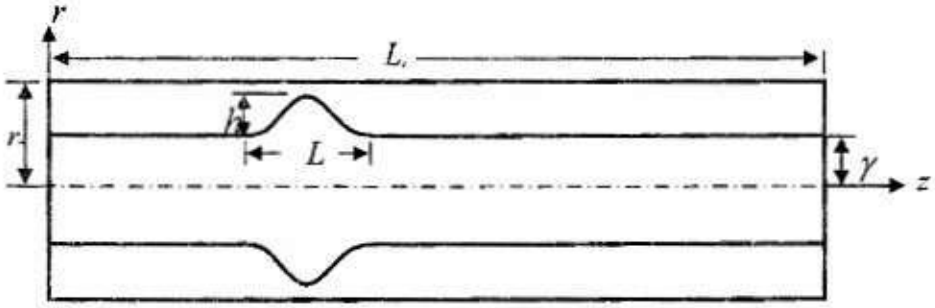

Fig. (1) Geometric representation of blocked annulus.

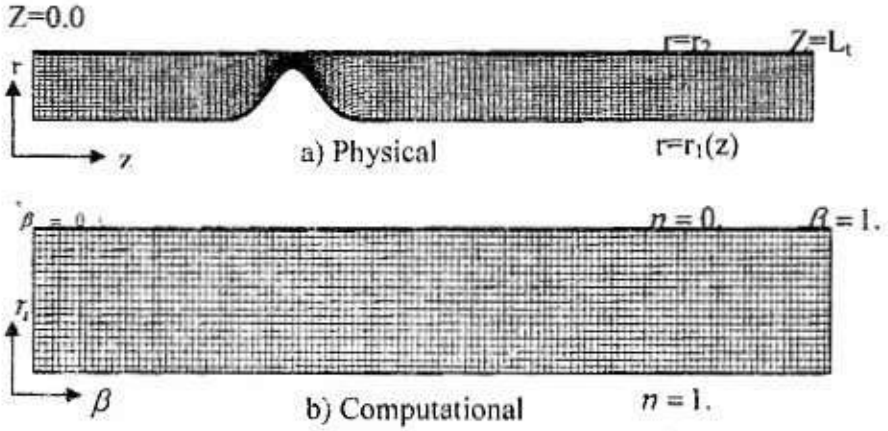

Fig. (2) Grid

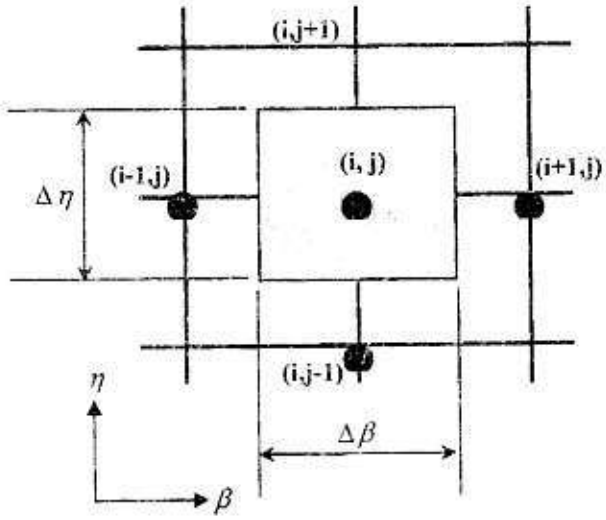

Fig.(3) Control volume.

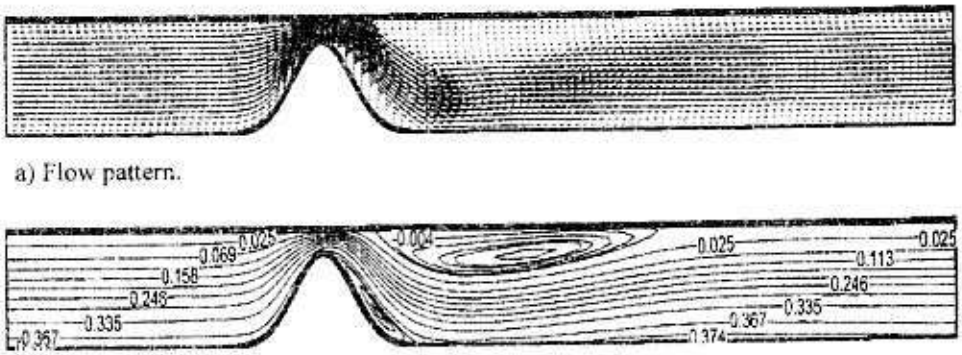

a) Flow pattern.

b) Streamlines pattern.

Fig. (4) Flow and streamlines patterns, Re=1000, h=0.4, L=1.0.

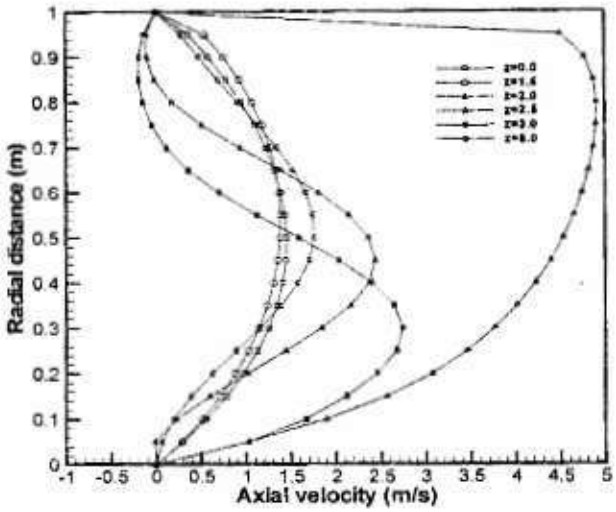

Fig. (5) Axial velocity profiles, Re=1000, h=0.4, L=1.0.

Fig. (6) Isotherms, Re=1000, h=0.4, L=1.0, insulated outer wall.

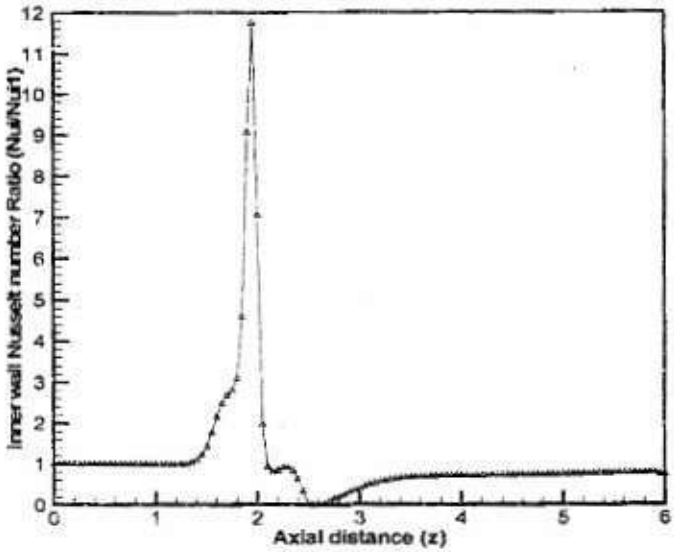

Fig. (7) Inner wall Nusselt number, Re=1000, Pr=1.0, h=0.4, L=1.0, insulated outer wall.

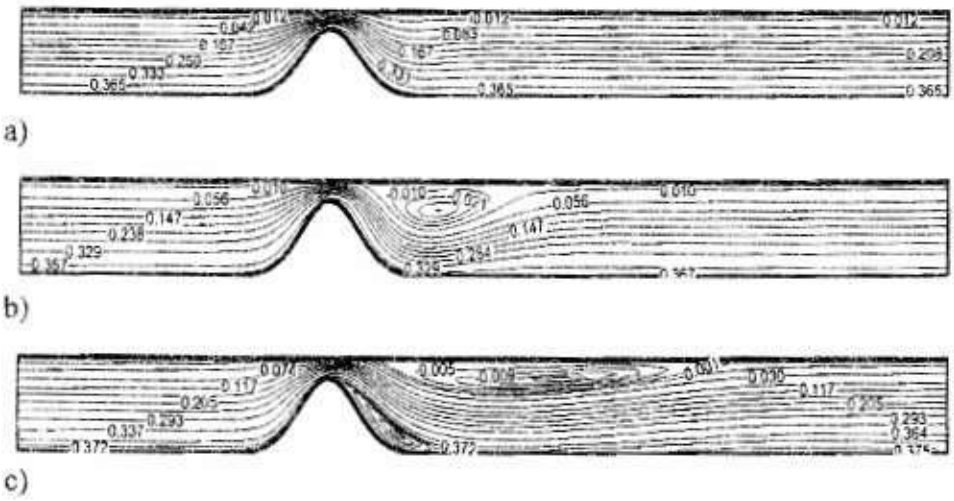

Fig. (8) Streamlines patterns: (a) Re=10, h=0.4, L=1.0: (b) Re=100, h=0.4, L=1.0: (c) Re=2000, h=0.4, L=1.0.

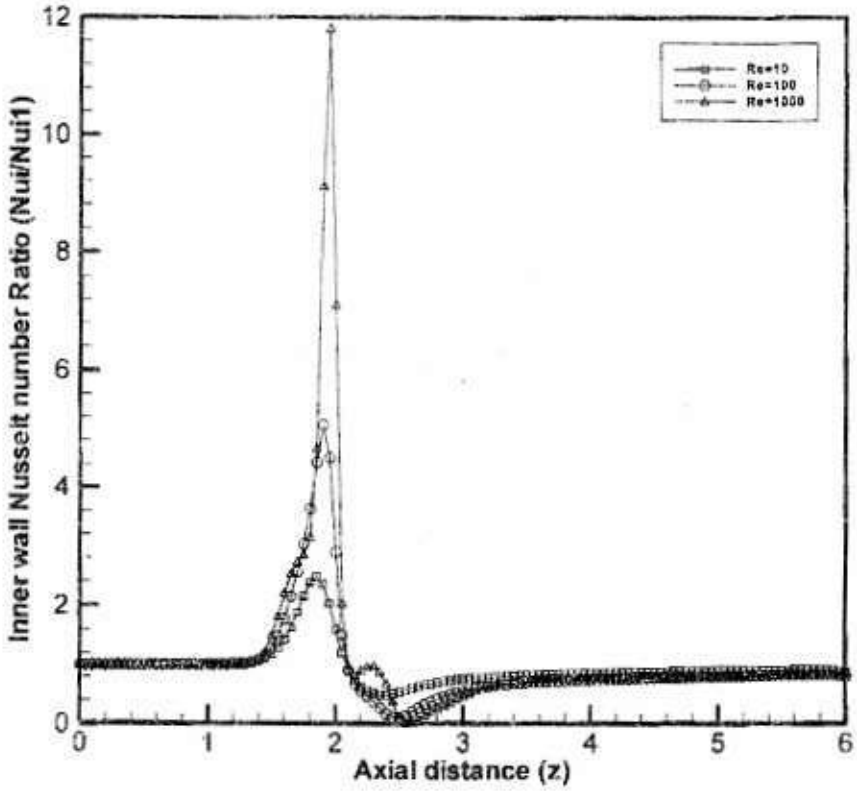

Fig. (9) Effect of Reynolds number on inner wall Nusselt number (Pr=1.0, h=0.4, L=1.0, insulated outer wall)

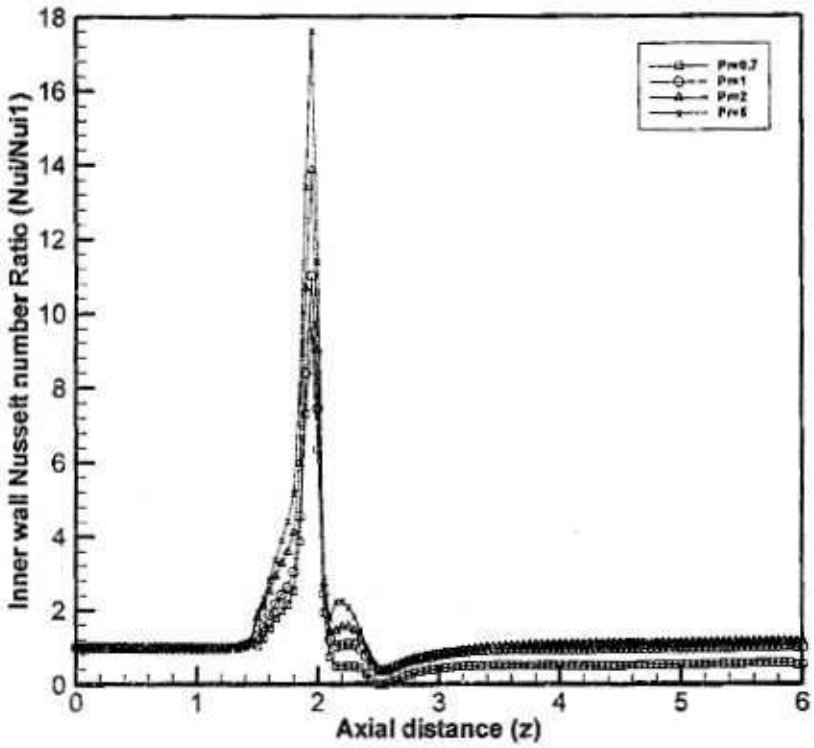

Fig. (10) Effect of Prandtl number on inner wall Nusselt number (Re=1000, h=0.4, L=1.0, insulated outer wall)

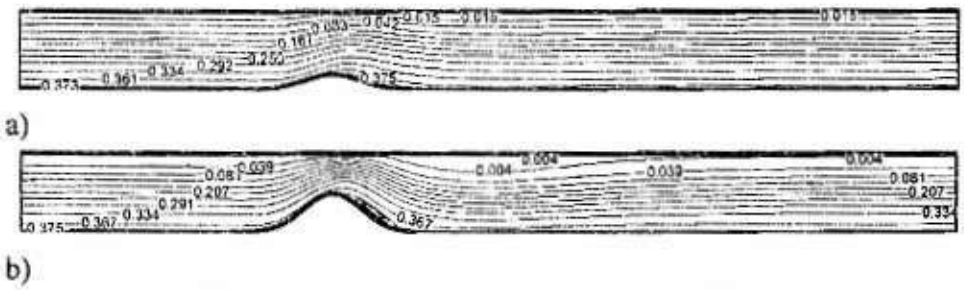

Fig. (11) Streamlines patterns: (a) Re=1000, h=0.1, L=1.0: (b) Re=1000, h=0.25, L=1.0.

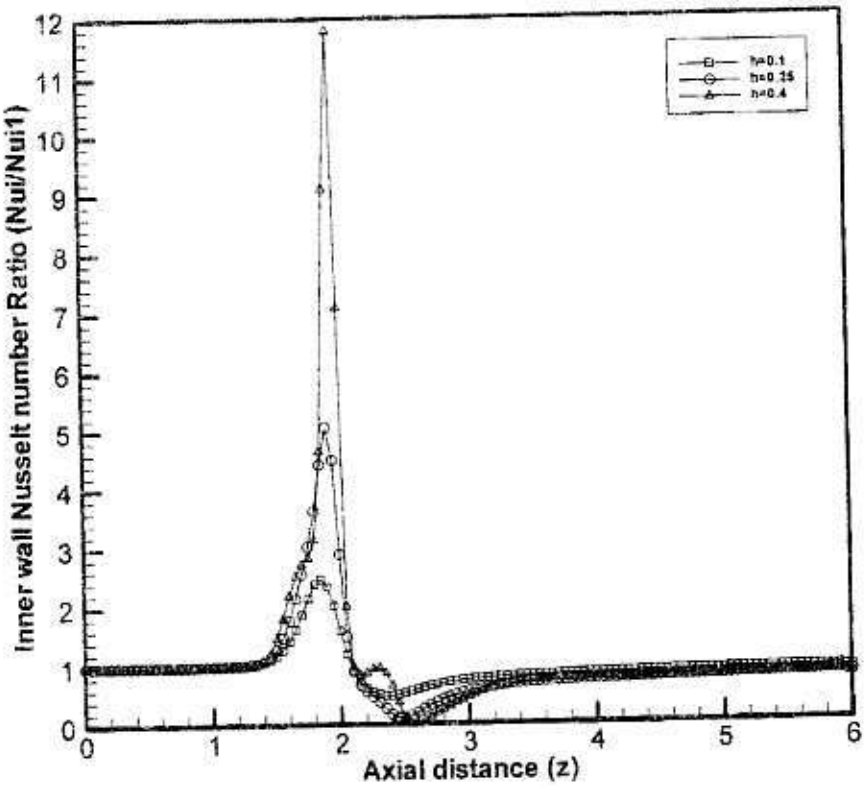

Fig. (12) Effect of blockage height on inner wall Nusselt number (Re=1000, Pr=1.0, L=1.0)